Research Square

Preprints are preliminary reports that have not undergone peer review.
They should not be considered conclusive, used to inform clinical practice,
or referenced by the media as validated information.

Altitudin S, an Antimicrobial Peptide Produced by Bacillus altitudinis ECC22, Defines a Novel Subgroup of Circular Bacteriocins

Ester Sevillano
Complutense University of Madrid
Irene Lafuente
Complutense University of Madrid
Nuria Peña
Complutense University of Madrid
Cleopatra Collado
Complutense University of Madrid
Luis Miguel Cintas
Complutense University of Madrid
Estefanía Muñoz-Atienza
Complutense University of Madrid
Pablo E. Hernández
Complutense University of Madrid
Juan Borrero
jborrero@ucm.es

Complutense University of Madrid

Research Article

Keywords: Bacillus altitudinis ECC22, altitudin S, circular bacteriocin, IV-CFPS/SIML, MALDI-TOF MS, LC-MS/MS

Posted Date: May 6th, 2026

DOI: https://doi.org/10.21203/rs.3.rs-9498654/v1

License: This work is licensed under a Creative Commons Attribution 4.0 International License.
Read Full License

Additional Declarations: No competing interests reported.

Abstract

Bacteriocins are ribosomally synthesized antimicrobial peptides with diverse structures and mechanisms of action. *Bacillus altitudinis* ECC22, previously shown to produce the circular bacteriocins pumilarin and altitudin A, was found to harbor an additional biosynthetic gene cluster encoding a novel circular bacteriocin, designated altitudin S. Proteomic analysis of purified active supernatant fractions confirmed the production of altitudin S, with a molecular mass of 8379 Da, consistent with head-to-tail cyclization. Altitudin S is synthesized as a 132-residue precursor comprising a 56-amino-acid leader and a 76-residue circular mature core. Structural modeling predicted a compact saposin-like fold composed of five α-helices and a strongly cationic surface (pI ≈ 11.0, net charge + 13). Altitudin S was also produced using an in vitro cell-free protein synthesis system coupled with split-intein mediated ligation (IV-CFPS/SIML) and exhibited a narrow but reproducible antimicrobial spectrum. Comprehensive sequence, structural, and phylogenetic analyses revealed that altitudin S is a highly divergent circular bacteriocin with distinctive sequence features and physicochemical properties, including an exceptionally high isoelectric point, strong cationic charge, and low hydrophobicity. Homologs were identified across diverse *Bacillales* species, displaying high sequence similarity, conserved structural features, and a shared physicochemical profile. Their biosynthetic gene clusters were also highly conserved and consistently encoded an M48-family metallopeptidase. Collectively, these findings support the classification of altitudin S and its homologs as representatives of a novel subgroup of circular bacteriocins.

1. Introduction

The increasing prevalence of antimicrobial resistance (AMR) represents a major global health challenge, compromising the efficacy of current antibiotics and severely limiting therapeutic options for bacterial infections [1]. Multidrug-resistant pathogens have emerged across clinical, agricultural, and environmental settings, further intensifying the urgent need for novel antimicrobial strategies [2]. Despite this demand, the discovery of new antibiotics has declined markedly in recent decades, hindered by scientific, economic, and regulatory constraints. Consequently, alternative approaches are receiving increasing attention, with bacteriocins emerging as promising candidates to combat resistant bacteria, either as standalone agents or in combination with conventional antibiotics [3].

Bacteriocins are ribosomally synthesized antimicrobial peptides produced by bacteria to inhibit the growth of closely related or competing bacterial species. They exhibit considerable structural diversity and a wide range of mechanisms of action, making them attractive candidates for both biotechnological and clinical applications. Bacteriocins are broadly classified into two major groups, among which class I bacteriocins, posttranslationally modified peptides, are of particular interest due to their structural complexity and functional diversity. Within this class, circular bacteriocins constitute a distinct subclass characterized by a head-to-tail cyclized backbone, a unique feature that confers exceptional stability, protease resistance, and tolerance to a wide range of pH values and elevated temperatures [4, 5].

Circular bacteriocins are typically divided into two main subgroups based on sequence characteristics and physicochemical properties. Subgroup I members typically consist of mature peptides of 60–70 amino acids with variable leader sequences (2–49 amino acids). They exhibit high isoelectric points (pI 9.5–10.5), net positive charges ranging from + 2 and + 6, high aliphatic indices (> 115), and moderately positive GRAVY values (0.5–1.1). These features promote strong electrostatic interactions with negatively charged bacterial membranes and facilitate membrane insertion and disruption. In contrast, subgroup II circular bacteriocins are shorter, with mature peptides of about 58 amino acids and leader sequences of 22–35 residues. They exhibit broader variability in pI (4.0–10.0), including neutral and negatively charged peptides, suggesting alternative mechanisms of action and target specificity. This diversity in charge and hydrophobicity reflects the evolutionary and functional heterogeneity within this group of antimicrobial peptides [6]. In addition to their structural and physicochemical diversity, circular bacteriocins are encoded within dedicated biosynthetic genetic clusters containing the genes required for synthesis, peptide maturation, transport, and immunity. A conserved feature of these clusters is the presence of the stage II sporulation protein M, a member of the DUF95 superfamily, which is thought to play a key role in peptide processing and cyclization [7]. Functionally, circular bacteriocins have been identified in a wide range of bacterial genera and exhibit potent antimicrobial activity against Gram-positive bacteria, including antibiotic-resistant pathogens [8].

In this study, we characterize a novel circular bacteriocin, altitudin S, produced by *Bacillus altitudinis* ECC22, a strain previously reported to synthetize two additional circular bacteriocins, pumilarin and altitudin A [9]. An integrated approach combining genome-based bioinformatic analysis, chromatographic purification, and mass spectrometry confirmed both the production and circular topology of altitudin S. In addition, altitudin S was produced using an in vitro cell-free protein synthesis (IV-CFPS) protocol coupled to a split intein-mediated ligation (SIML) platform [10], followed by evaluation of its antimicrobial activity. Phylogenetic and structural analyses identified altitudin S as a distinct circular bacteriocin with unique sequence features and physicochemical properties. Homologs were identified across diverse *Bacillales* species, exhibiting conserved structural features including a five-helix fold, and similar physicochemical properties. Their biosynthetic gene clusters were also highly conserved and consistently encoded an M48 family metallopeptidase. Collectively, these findings support the classification of altitudin S as the prototype of a novel subgroup of circular bacteriocins. This study expands the known diversity of circular bacteriocins and highlights the potential of altitudin S for future biotechnological and antimicrobial applications.

2. Material and methods

2.1. Bacterial isolate and bacteriocin mining

The soil-derived strain *B. altitudinis* ECC22 was originally isolated from soil samples collected by high school students participating in the Micromundo citizen science project [11, 12]. This strain was previously shown to produce the circular bacteriocins pumilarin and altitudin A [9]. To extend these findings, a more comprehensive re-analysis of its genome (GenBank accession number CP137888) was

performed using antiSMASH (https://antismash.secondarymetabolites.org/, accessed on 13 January 2025) [13]. Additional analyses were performed using BLASTp (NCBI) and UniProt for peptide comparisons, and SnapGene 6.2.1. (GSL Biotech, San Diego, CA, USA) for the annotation and characterization of bacteriocin biosynthetic gene clusters (BGCs).

2.2. MALDI-TOF MS and LC-MS/MS analysis of purified supernatants from *B. altitudinis* ECC22

Bacteriocins were purified from the cell-free supernatant (CFS) of *B. altitudinis* ECC22 using a multi-step chromatographic procedure [9]. Cultures were grown for 24 h in Brain Heart Infusion (BHI) broth (Oxoid Ltd., Basingstoke, UK) at 32°C with agitation at 250 rpm in an orbital shaker (Ecotron, Infors HT, Braunschweig, Germany). The purified CFS fraction obtained from the final RP-FPLC chromatographic step exhibiting antimicrobial activity was analyzed by MALDI-TOF MS to determine peptide molecular masses. In addition, this fraction was subjected to LC-MS/MS analysis to determine the amino acid sequences of the resulting trypsin-digested peptides at the Unidad de Espectrometría de Masas (CAI Técnicas Biológicas, UCM, Madrid, Spain), as previously described [9].

2.3. IV-CFPS/SIML for production of altitudin S and evaluation of its antimicrobial activity

For in vitro production and circularization of altitudin S, synthetic gene constructs were designed in which the 76-amino acid sequence of mature altitudin S was flanked by the C-terminal (I_C, 37 amino acids) and N-terminal (I_N, 88 amino acids) fragments of the split Gp41-1 intein (Supplementary Fig. S1), as previously described [10]. Six constructs were generated, each incorporating a different serine residue as the + 1 position required for intein-mediated splicing. In all cases, the residue immediately preceding the selected serine was positioned at the C-terminus of the peptide, adjacent to the I_N fragment. Sequences were reverse-translated according to *Escherichia coli* codon usage using the GeneArt Gene Synthesis tool (Thermo Fisher Scientific) and cloned into a pUC-derived expression vector under the control of a T7 promoter and terminator (Supplementary Fig. S1). The constructs were designated as pCirc-AltS-S9, pCirc-AltS-S22, pCirc-AltS-S32, pCirc-AltS-S39, pCirc-AltS-S46, and pCirc-AltS-S60.

Plasmids were obtained from GeneArt (Thermo Fisher Scientific) and used as templates for IV-CFPS/SIML reactions using the PURExpress In Vitro Protein Synthesis Kit (New England Biolabs, Ipswich, MA, USA), following established protocols [10, 14, 15]. Reactions were performed using plasmid DNA templates at a final concentration of 10 ng/µL, incubated at 37°C for 2 h, and subsequently maintained at room temperature overnight to allow intein-mediated splicing and peptide circularization.

Antimicrobial activity of the IV-CFPS/SIML products was assessed by spot-on-agar test (SOAT), as previously described [14]. Briefly, 5 µL aliquots of twofold serial dilutions were spotted onto Man, Rogosa and Sharpe (MRS) agar (1.5% w/v) overlaid with MRS soft agar (0.8% w/v) seeded with *Pediococcus damnosus* CECT 4797 (~ 10^5 CFU/mL). Plates were incubated at 32°C overnight until inhibition zones

were observed. For assays using pCirc-AltS-S60-derived products, incubation conditions were adjusted according to each indicator strain (Supplementary Table S1).

2.4. Bioinformatic analyses of altitudin S and homologs

2.4.1. Identification of homologs

Homologs of altitudin S were identified by querying the mature peptide sequence against the NCBI database using BLASTp. Sequences with 100% query coverage were considered putative homologs or variants.

2.4.2. Sequence alignment and phylogenetic analysis

To assess evolutionary relationships, altitudin S and its homologs were aligned together with representative circular bacteriocins using Clustal Omega (EMBL-EBI) with default parameters in the Jalview 2.11.4.1 [16]. A neighbor-joining phylogenetic tree was generated in Jalview using the BLOSUM62 substitution matrix and visualized with Interactive Tree of Life (iTOL, https://itol.embl.de).

2.4.3. Physicochemical properties calculations

The physicochemical properties of altitudin S and its homologs were computed using the ProtParam tool (ExPASy) [17]. Parameters included molecular mass (corrected by subtracting 18 Da to account for water loss during cyclization), theoretical isoelectric point (pI), net charge at pH 7.0, aliphatic index, and grand average of hydropathy (GRAVY). These parameters provide insight into peptide stability, hydrophobicity, and electrostatic properties, which are key determinants of antimicrobial activity and membrane interaction.

2.4.4. Structural modeling

The three-dimensional (3D) structures of altitudin S and its homologs was predicted using AlphaFold [18] and visualized with ChimeraX [19].

2.4.5. Genomic context analysis

Genomic regions encoding altitudin S homologs were analyzed using antiSMASH, supported by BLASTp (NCBI) and UniProt for sequence comparisons, and SnapGene 6.2.1 for annotation and visualization of bacteriocin BGCs.

3. Results

3.1. Genomic features of the altitudin S biosynthetic gene cluster

B. altitudinis ECC22 harbors a circular chromosome of 3,807,059 bp (GenBank accession number CP137888) and was previously reported to encode three BGCs corresponding to pumilarin, altitudin A,

and a putative closticin 574-like peptide [9]. Of these, pumilarin and altitudin A were experimentally validated, whereas the closticin 574-like cluster remained uncharacterized. However, a more detailed re-analysis of the genome identified an additional, previously overlooked BGC predicted to encode a novel circular bacteriocin, which we designated altitudin S.

The predicted precursor of altitudin S is a 132-amino acid peptide encoded within a gene cluster that also includes genes for ABC transporter proteins, a stage II sporulation protein M (SpoIIM) of the DUF95 superfamily, and a YIP1 family membrane protein (Fig. 1), all characteristic components of circular bacteriocin BGCs. The overall organization of this cluster closely resembles that of the pumilarin and altitudin A clusters; however, a key distinction is the presence of an additional gene encoding a predicted M48 family metallopeptidase, which is absent from the other two clusters. This unique feature points to a potentially distinct mechanism of leader peptide processing or maturation in altitudin S.

Figure 1 Genomic organization of the altitudin S BGC compared with those of pumilarin and altitudin in *B. altitudinis* ECC22. Genes are color-coded according to predicted function.

3.2. MALDI-TOF MS and LC-MS/MS analyses of purified bacteriocins produced by *B. altitudinis* ECC22

Purification of the CFS of *B. altitudinis* ECC22 by multi-step chromatography, followed by MALDI-TOF MS analysis of the most active RP-FPLC fraction, revealed three major peptides with molecular masses of 6598.9, 7089.1, and 8381.9 Da, corresponding to altitudin A, pumilarin, and the novel peptide altitudin S, respectively (Fig. 2). For altitudin S, the observed mass was 18 Da lower than the theoretical molecular mass (8397.0 Da), consistent with a dehydration event resulting from amide bond formation between the N- and C-termini and subsequent peptide cyclization. Similar mass differences were observed for altitudin A (6615.9 vs. 6598.9 Da) and pumilarin (7105.4 vs. 7089.1 Da), confirming that all three peptides undergo head-to-tail cyclization in *B. altitudinis* ECC22.

Targeted LC–MS/MS analysis of trypsin-digested peptides from the purified CFS further confirmed the identity of altitudin S. Two peptides, TTWNQAQK and AAVTWLAK, were unambiguously assigned to the predicted mature sequence (Supplementary Table S2). Notably, detection of AAVTWLAK, spanning residues L1 and W76, confirmed the head-to-tail cyclization junction, providing definitive evidence of altitudin S production by *B. altitudinis* ECC22. Collectively, these results indicate that altitudin S is synthesized as a 132-amino acid precursor that undergoes proteolytic removal of a 56-amino acid peptide to yield a 76-amino acid mature circular bacteriocin (Fig. 3A).

3.3. Physicochemical profile and predicted 3D structure of altitudin S

From the ProtParam evaluation of the physicochemical properties of altitudin S, the peptide is predicted to be a highly cationic peptide, with a theoretical pI of 11.0, and a net positive charge of + 13, arising from 14 basic residues (2 arginines and 12 lysines) and a single acidic residue. The peptide also exhibits

an aliphatic index of 90.0 and a nearly-neutral GRAVY score of 0.025. Collectively, these features indicate moderate hydrophobicity combined with a strongly positive electrostatic profile, characteristics commonly associated with antimicrobial activity.

Structural modeling using AlphaFold predicted that altitudin S adopts a saposin-like fold, consisting of five α-helices arranged in a compact circular conformation (Fig. 3B). Electrostatic surface analysis revealed a pronounced positive charge distribution, consistent with its predicted physicochemical properties and likely important for interactions with negatively charged bacterial membranes.

3.4. IV-CFPS/SIML synthesis and antimicrobial activity of altitudin S

As altitudin S could not be purified to homogeneity from the CFS of *B. altitudinis* ECC22 (Fig. 2), an IV-CFPS/SIML approach was employed for its production, following previously described protocols from our research group [9, 10, 15]. Six pUC-derived constructs were generated, each incorporating a different serine residue as the + 1 position required for Gp41-1 intein-mediated splicing. This strategy enabled efficient production and head-to-tail cyclization of altitudin S, allowing functional validation. Among the constructs tested (pCirc-AltS-S9, pCirc-AltS-S22, pCirc-AltS-S32, pCirc-AltS-S39, pCirc-AltS-S46 and pCirc-AltS-S60), pCirc-AltS-S60 produced the largest inhibition zones, indicating the highest antimicrobial activity (Supplementary Fig. S2).

Altitudin S obtained from the pCir-AltS-S60 construct displayed antimicrobial activity against a limited panel of indicator strains, consistent with a narrow spectrum predominantly targeting Gram-positive bacteria. No activity was detected against Gram-negative strains, including *Escherichia coli*, *Salmonella* spp., *Pseudomonas aeruginosa*, *Acinetobacter baylyi*, *Fusobacterium nucleatum*, and *Porphyromonas gingivalis*. Among Gram-positive bacteria, several species were not inhibited under the conditions tested; however, clear activity was detected against *P. damnosus*, *Listeria* species (*L. monocytogenes*, *L. innocua*, and *L. seeligeri*), *Bacillus* species (*B. pumilus*, *B. safensis*, and *B. cereus*), and selected *Paenibacillus* species (*P. larvae* and *P. lentus*). Activity was also observed against *Kocuria rhizophila*. Overall, altitudin S exhibited a narrow antimicrobial spectrum, primarily targeting selected Gram-positive taxa, particularly members of the genera *Listeria*, *Bacillus*, and *Paenibacillus* (Table 1; Supplementary Fig. S3).

Table 1
Antimicrobial activity of IV-CFPS/SIML-produced altitudin S derived from the pCir-AltS-S60 construct, evaluated by spot-on-agar test (SOAT) against selected Gram-positive indicator strains.

Strain	**Antimicrobial activity[a]**
Escherichia coli DH5α	-
Salmonella paratyphi CECT 554	-
Salmonella Cholerasuis ZTA18/02215	-
Pseudomonas aeruginosa CECT 108	-
Acinetobacter baylyi ATCC 33305	-
Fusobacterium nucleatum DSMZ 20482	-
Porphyromonas gingivalis ATCC 33277	-
Staphylococcus aureus ZTA11/00117ST	-
Staphylococcus aureus DICM10/00243	-
Enterococcus faecium ER46	-
Enterococcus faecalis 12Ep11	-
Lactococcus garvieae CECT 5806	-
Lactococcus lactis IL1403	-
Pediococcus damnosus CECT 4797	10.6
Pediococcus pentosaceus FBB61	-
Listeria monocytogenes CECT 4032	8.2
Listeria innocua CECT 910	9.5
Listeria seeligeri CECT 917	8.0
Bacillus pumilus PE12	8.6
Bacillus safensis LTh12	8.0
Bacillus cereus CM7	7.8
Bacillus toyonensis NM11	-
Paenibacillus larvae DB25	9.8
Paenibacillus dendritiformis P1CEA1	-
Paenibacillus lentus P8CEA5	8.2
Paenibacillus polymyxa SFU2431	-

Strain	Antimicrobial activity[a]
Kocuria rhizophila CECT 241	8.0
Streptococcus suis CECT 958	-
Streptococcus agalactiae ICM21/01900	-
Streptococcus mutans ATCC 25175	-
Clostridium perfringens DICM15/00067-5A	-
Erysipelothrix rhusiopathiae ICM21/01900	-
Corynebacterium pseudotuberculosis Cam2	-
Trueperella pyogenes ICM17/02091-1	-

[a] Samples showing a clear halo of inhibition (mm) or no detectable inhibition (-).

3.5. Identification of altitudin S homologs

BLASTp analysis using the mature sequence of altitudin S as a query identified multiple homologs across diverse *Bacillales* species, including *B. altitudinis*, *Bacillus pumilus*, *Aeribacillus alveayuensis*, *Evansella* spp., *Siminovitchia sediminis*, and *Caldalkalibacillus mannanilyticus* (Fig. 4). All homologs exhibited 100% query coverage and ranged from 75 to 82 amino acids (8307–9311 Da). Despite sequence variability, they consistently displayed the distinctive physicochemical profile of altitudin S, characterized by highly basic pI values (10.3–11.0), strong cationic charges (+ 7 to + 13), and low or near-neutral hydrophobicity (GRAVY − 0.177 to 0.272) (Supplementary Table S3).

Predicted 3D structures of these homologs revealed a conserved compact globular fold comprising five α-helices, consistent with the structural scaffold of altitudin S (Supplementary Fig. S4). This conservation indicates that, despite some sequence divergence, the overall tertiary structure is preserved.

Comparative genomic analysis of the BGCs encoding altitudin S and its homologs showed a highly conserved organization. Each cluster included the structural gene for the precursor peptide, a YIP1 family membrane protein, a SpoIIM protein (DUF95 superfamily), and ABC transporter subunits (Supplementary Fig. S5). A distinctive hallmark of the altitudin S cluster, shared across all homologs, was the presence of an M48 family metallopeptidase gene located within the gene cluster, downstream of the structural gene. This protease is absent from previously characterized circular bacteriocin clusters, such as those encoding pumilarin and altitudin A [9], which otherwise share conserved elements including ABC transporters and SpoIIM.

3.6. Comparative analysis of altitudin S-like homologs with characterized circular bacteriocins

Comparison of the mature amino acid sequences of altitudin S and its homologs with those of characterized circular bacteriocins revealed limited similarity to either subgroup I (e.g., garvicin ML, enterocin AS-48, circularin A, altitudin A, pumilarin) or subgroup II (e.g., plantaricyclin A, plantacyclin B21AG, acidocin B, paracyclicin). Multiple sequence alignment identified distinct sequence features that differentiate altitudin S and its homologs from both canonical subgroups. Notably, these features include an extended N-terminal motif (LAKITNK…) and a high frequency of lysine residues throughout the sequence, contributing to the pronounced cationic character of this group (Fig. 4). Together, these characteristics diverge from the conserved sequence signatures of subgroup I and II bacteriocins, supporting the classification of altitudin S-like peptides as a structurally and functionally distinct lineage of circular bacteriocins.

Phylogenetic analysis of altitudin S, its homologs, and representative circular bacteriocins confirmed their distinct evolutionary divergence. Altitudin S and its homologs formed a separate clade, clearly segregated from the established subgroup I and II clusters (Fig. 5). The extended branch length of this clade indicates substantial evolutionary distance, supporting its classification as an independent lineage within the circular bacteriocin family.

The physicochemical properties of the altitudin S-like peptides differ markedly from those of previously described circular bacteriocins. Members of subgroup I typically comprise 60–70 amino acids, exhibit highly basic pI values (9.5–10.5), moderate hydrophobicity (GRAVY 0.5–1.1), and net positive charges ranging from + 2 to + 6. In contrast, subgroup II members are shorter (≈ 58 amino acids) and display greater variability in charge and hydropathy, including neutral or negatively charged representatives (Supplementary Table S4). Altitudin S-like peptides deviate from both groups, as they are longer (75–82 amino acids), exhibit extremely high theoretical pI values (10.3–11.0), unusually high net positive charges (+ 7 to + 13), and near-neutral GRAVY values (Supplementary Table S3). These features highlight their pronounced basicity and relatively low hydrophobicity.

4. Discussion

The global rise in AMR represents a major threat to public health, underscoring the urgent need for new antimicrobial agents. Bacteriocins, particularly circular bacteriocins, have attracted considerable attention due to their stability and potential as alternative antimicrobial agents [7]. Here, we report the identification and characterization of a novel circular bacteriocin, altitudin S, produced by *B. altitudinis* ECC22, a strain previously reported to produce the circular bacteriocins pumilarin and altitudin A [9]. These findings further support *Bacillus* sp. as a valuable source of antimicrobial peptides [20].

A more comprehensive re-analysis of the *B. altitudinis* ECC22 genome identified a third BGC predicted to encode a putative novel circular bacteriocin, altitudin S, in addition to those responsible for pumilarin and altitudin A. Examination of the altitudin S BGC revealed conserved features typical of circular bacteriocin operons, including genes encoding the precursor peptide, a SpoIIM protein (DUF95 superfamily), a YIP1 family membrane protein, and a two-component ABC transporter (Fig. 1). This organization is highly

conserved among circular bacteriocin gene clusters [21] and is also observed in pumilarin and altitudin A clusters, indicating a shared biosynthetic framework. However, a distinguishing feature of the altitudin S cluster is the presence of a gene encoding an M48 family metallopeptidase located within the gene cluster. This protease, absent from the pumilarin and altitudin A clusters, suggests a potential role in precursor processing and points to a specialized maturation pathway. Although the mechanisms of leader peptide cleavage and core peptide cyclization remain elusive, further experimental studies are required to elucidate the roles of the enzymes, as well as additional factors encoded elsewhere in the genome [6, 21]. Notably, many class I circular bacteriocin BGCs contain an accessory operon of three to four genes encoding a putative ABC transporter complex, typically encoding a permease, an ATP-binding protein, and a predicted extracellular component, as described for enterocin AS-48 (AS-48EFGH). However, functional studies suggest that this complex has no significant impact on bacteriocin production or immunity [8]. Consistent with this variability, the altitudin S gene cluster lacks a dedicated immunity gene, a feature also observed in several other circular bacteriocin clusters [22, 23].

Production of altitudin S by *B. altitudinis* ECC22 was confirmed by purification of the CFS and MALDI-TOF MS analysis of active fractions. The observed molecular masses for altitudin A, pumilarin, and altitudin S were ~ 18 Da lower than their theoretical values, consistent with dehydration associated with head-to-tail cyclization (Fig. 2). LC–MS/MS analysis of tryptic fragments identified TTWNQAQK and AAVTWLAK, both mapping to the predicted mature sequence. Notably, detection of AAVTWLAK, spanning residues L1 and W76, provided direct evidence of head-to-tail circularization of altitudin S in the native producer. These proteomic data, together with genomic analysis, demonstrate that altitudin S is synthesized as a 132-amino acid precursor comprising a 56-amino acid leader sequence and a 76-amino acid core peptide. Following leader peptide cleavage and ligation of residues L1 and W76, the mature bacteriocin is formed (Fig. 3A). Altitudin S represents the largest circular bacteriocin described to date, with both its core peptide and leader sequence exceeding the typical size ranges reported for this class (58–70 and 2–48 residues, respectively) [8]. Remarkably, altitudin S also displays unusual physicochemical properties, including a theoretical pI of 11.0 and a net charge of + 13, placing it among the most cationic circular bacteriocins reported to date (Supplementary Table S3). Structural predictions further suggests that, like most circular bacteriocins, altitudin S adopts a compact saposin-like fold composed of five α-helices, with the cyclization site buried within a sterically constrained hydrophobic α-helix (Fig. 3B) [20]. This arrangement likely stabilizes the circular structure and promotes membrane disruption through ion leakage, dissipation of membrane potential, and ultimately cell death [7, 20].

However, given the uncertainty associated with obtaining purified altitudin S using multi-step chromatographic procedures, an IV-CFPS/SIML approach, previously developed by our group, was employed for the in vitro synthesis, cyclization and functional expression of altitudin S [9, 10, 15]. Intein-mediated splicing efficiency is strongly influenced by the identity of the flanking extein residues and is optimal when a nucleophilic residue (typically Cys, Ser, or Thr) occupies the + 1 position, as its steric and electronic properties govern the trans-(thio)esterification reaction underlying peptide bond formation. Accordingly, six pUC-derived constructs were generated, each incorporating a different serine at the + 1 position required for Gp41-1 intein-mediated splicing (Supplementary Fig. S1). This strategy enabled

efficient production and head-to-tail cyclization of altitudin S, allowing functional validation. Among the constructs tested, pCirc-AltS-S60 produced the largest inhibition zones, indicating the highest antimicrobial activity (Supplementary Fig. S2).

Altitudin S produced from the pCir-AltS-S60 construct exhibited antimicrobial activity against a limited panel of indicator strains (Table 1; Supplementary Fig. S3). Its activity was primarily directed toward selected Gram-positive taxa, particularly members of the genera *Listeria*, *Bacillus*, and *Paenibacillus*, while most other Gram-positive bacteria tested, including *Enterococcus*, *Streptococcus*, and *Lactococcus*, were not affected under the conditions evaluated. This narrow spectrum resembles that of altitudin A, in contrast to the broader activity of pumilarin [9], likely reflecting differences in peptide charge distribution and other factors influencing bacteriocin–membrane interactions and target cell susceptibility [6]. These findings further highlight the utility of IV-CFPS/SIML-based systems as a powerful tool for the production and characterization of circular bacteriocins that are difficult to purify from native sources. However, a limitation of this approach is that the concentration of the synthesized peptide remains unknown and may be insufficient to fully assess its antimicrobial potential. Further studies using higher and accurately quantified peptide concentrations will be required to better define the activity and inhibitory spectrum of altitudin S.

The identification of altitudin S homologs across diverse bacterial genera, including *Bacillus*, *Evansella*, and *Caldalkalibacillus*, suggest that these bacteriocins are more widely distributed than previously anticipated. These homologs share the distinctive properties of altitudin S, including extended mature peptides (75 to 82 amino acids), high pI and strong cationic charge, near-neutral hydrophobicity, a conserved five-helix saposin-like fold, and a similar BGC organization (Supplementary Fig. S4, Supplementary Fig. S5, and Supplementary Table S3). Taken together, these conserved sequence, structural, and genomic features indicate that altitudin S-like bacteriocins may represent a coherent lineage within the circular bacteriocin family.

Comparative sequence and phylogenetic analyses further support this conclusion. Despite the presence of some conserved motifs, altitudin S-like peptides show limited similarity to circular bacteriocin subgroups I and II (Fig. 4). In phylogenetic trees, they consistently clustered together but branched separately, giving rise to a long, independent lineage (Fig. 5). The basal branching pattern and substantial evolutionary distance suggest that these peptides may have originated from an early divergent event or followed an independent evolutionary trajectory relative to other circular bacteriocins [6, 8, 24].

Moreover, their predicted physicochemical and genomic features further support this distinction. Subgroup I bacteriocins are typically moderately hydrophobic and cationic (net charge + 2 to + 6; pI ~ 10), while subgroup II members are shorter (58 amino acids) and display greater variability in charge and hydropathy [6]. In contrast, altitudin S and its homologs consistently exhibit high theoretical pI values (10.3–11.0), strong net positive charges (+ 7 to + 13), and near-neutral GRAVY values, placing them at the upper range of cationicity reported for circular bacteriocins [6, 8, 24]. This profile suggests that

classical hydrophobic pore formation may be less favored and that antimicrobial activity may instead rely on electrostatic interactions with negatively charged bacterial membranes, potentially leading to surface-associated membrane destabilization rather than stable pore insertion. Such a mechanism is consistent with the two-step model proposed for antimicrobial peptides [25], as well as with evidence indicating that many cationic peptides disrupt membranes via transient leakage and interfacial activity rather than forming stable pores [25–27]. Further biophysical studies will be needed to validate the precise mode of action of altitudin S-like bacteriocins.

Comparative genomic analysis revealed that altitudin S and its homologs share a conserved operon structure, including the structural gene, ABC transporter subunits, a SpoIIM protein, and a YIP1 family membrane protein, but are consistently distinguished by the presence of an M48 metallopeptidase located two genes downstream of the precursor gene (Supplementary Fig. S5). Together with their unusually long leader and mature peptides, this feature strongly suggests that altitudin S-like bacteriocins may undergo a specialized maturation pathway distinct from that of other circular bacteriocins. Given that M48 metallopeptidases are associated with intramembrane proteolysis and peptide processing [21], their conserved presence across homologous clusters points to additional or alternative posttranslational processing steps. These findings highlight new avenues for investigating the biosynthesis and functional diversification of this novel subgroup of circular bacteriocins.

5. Conclusions

By integrating genomic mining, multi-step purification, mass spectrometry (MALDI-TOF MS, LC–MS/MS), and synthetic biology approaches (IV-CFPS/SIML), we identified and characterized a novel circular bacteriocin, altitudin S, produced by *B. altitudinis* ECC22. Altitudin S is distinguished by its unusual physicochemical profile, clear phylogenetic separation from previously described circular bacteriocins, and a distinctive biosynthetic gene cluster architecture. The identification of closely related homologs across diverse bacterial genera further supports the classification of altitudin S-like peptides as a distinct and previously unrecognized lineage within the circular bacteriocin family. These findings expand the known diversity of circular bacteriocins and highlight their broad taxonomic distribution and potential ecological and biotechnological significance.

Declarations

Credit authorship contribution statement

Conceptualization, E.M.-A., P.E.H. and J.B.; methodology, E.S., N.P., I.L., C.C., P.E.H. and J.B.; investigation, E.S., N.P., I.L., C.C., E.M.-A. and J.B.; resources, L.M.C., E.M.-A., P.E.H. and J.B.; data curation, E.S., P.E.H. and J.B.; writing—original draft preparation, E.S.; writing—review and editing, P.E.H. and J.B.; supervision, E.M.-A., P.E.H. and J.B.; project administration, J.B. and E.M.-A.; funding acquisition, L.M.C., P.E.H. and J.B. All authors have read and agreed to the published version of the manuscript.

Funding

This work was supported by the Ministerio de Ciencia e Innovación (PID2019-104808RA-I00; CNS2023-144585; PID2023-150939OB-I00), the Atracción de Talento Program of the Comunidad de Madrid (2018-T1/BIO-10158; 2022-5A/BIO-24232) and the UCM Service-Learning program (2021-2022). I.L., N.P., and J.B. were supported by the Atracción de Talento Program of the Comunidad de Madrid (2018-T1/BIO-10158; 2022-5A/BIO-24232). E.S. was supported by the Empleo Juvenil Program of the Comunidad de Madrid (PEJ-2020-AI/BIO-17758) and the Ministerio de Ciencia e Innovación (PID2019-104808RA-I00; CNS2023-144585). C.C. was supported by the Ministerio de Ciencia e Innovación (PID2023-150939OB-I00).

Declaration of competing interest

The authors declare no known competing financial interests or personal relationships that could have influenced the work reported in this article.

Ethical approval

This study did not involve human participants or vertebrate animals. All sampling procedures complied with the Nagoya Protocol (reference ABSCH-IRCC-ES-270144-1).

Data availability

The whole-genome assembly of *B. altitudinis* ECC22 has been deposited in GenBank under accession number CP137888.

Acknowledgments

We gratefully acknowledge the Micromundo project at the Universidad Complutense de Madrid and the participating high-school students from IES El Cantizal (Las Rozas, Madrid), under the guidance of their teacher Alicia Cuartero, for their contribution to the isolation of *B. altitudinis* ECC22. We also thank the project coordinators, Prof. Víctor Jiménez-Cid and Prof. Jessica Gil-Serna, for leading the Micromundo initiative. We further acknowledge the Proteomics Unit of the University Complutense of Madrid (UCM) for technical assistance with proteomic analysis.

Appendix A. Supplementary data

Supplementary material associated with this article (Table S1, Table S2, Table S3, Table S4, and Fig. S1, Fig. S2, Fig. S3, Fig. S4, and Fig. S5) can be found, in the online version, at ----------

Declaration of generative AI and AI-assisted technologies in the manuscript preparation process

During the preparation of this manuscript, the authors used ChatGPT (GPT-5, OpenAI) to assist with improving clarity, grammar, and overall readability, as well as to refine wording for conciseness. All content generated with the assistance of this tool was critically reviewed, edited, and validated by the authors, who take full responsibility for the accuracy, integrity, and originality of the final manuscript.

References

1. Murray CJ, Ikuta KS, Sharara F et al (2022) Global burden of bacterial antimicrobial resistance in 2019: a systematic analysis. Lancet 399:629–655. https://doi.org/10.1016/S0140-6736(21)02724-0
2. Reygaert WC, Reygaert WC (2018) An overview of the antimicrobial resistance mechanisms of bacteria. AIMS Microbiology 2018 3:482 4:482–501. https://doi.org/10.3934/MICROBIOL.2018.3.482
3. Cotter PD, Ross RP, Hill C (2012) Bacteriocins — a viable alternative to antibiotics? Nature Reviews Microbiology 2012 11:2 11:95–105. https://doi.org/10.1038/nrmicro2937
4. Montalbán-López M, Scott TA, Ramesh S et al (2021) New developments in RiPP discovery, enzymology and engineering. Nat Prod Rep 38:130–239. https://doi.org/10.1039/D0NP00027B
5. Ongpipattanakul C, Desormeaux EK, Dicaprio A et al (2022) Mechanism of Action of Ribosomally Synthesized and Post-Translationally Modified Peptides. Chem Rev 122:14722. https://doi.org/10.1021/ACS.CHEMREV.2C00210
6. Gabrielsen C, Brede DA, Nes IF, Diep DB (2014) Circular Bacteriocins: Biosynthesis and Mode of Action. Appl Environ Microbiol 80:6854. https://doi.org/10.1128/AEM.02284-14
7. Liu F, van Heel AJ, Kuipers OP (2024) Engineering circular bacteriocins: structural and functional effects of α-helix exchanges and disulfide introductions in circularin A. Front Microbiol 15:1337647. https://doi.org/10.3389/FMICB.2024.1337647
8. Perez RH, Zendo T, Sonomoto K (2018) Circular and leaderless bacteriocins: Biosynthesis, mode of action, applications, and prospects. Front Microbiol 9:410161. https://doi.org/10.3389/FMICB.2018.02085
9. Lafuente I, Sevillano E, Peña N et al (2024) Production of Pumilarin and a Novel Circular Bacteriocin, Altitudin A, by Bacillus altitudinis ECC22, a Soil-Derived Bacteriocin Producer. Int J Mol Sci 25:2020. https://doi.org/10.3390/IJMS25042020
10. Peña N, Bland MJ, Sevillano E et al (2022) In vitro and in vivo production and split-intein mediated ligation (SIML) of circular bacteriocins. Front Microbiol 13. https://doi.org/10.3389/FMICB.2022.1052686
11. Gil-Serna J, Antunes P, Campoy S et al (2025) Citizen Science to Raise Antimicrobial Resistance Awareness in the Community: The MicroMundo Project in Spain and Portugal. Microb Biotechnol 18:e70123. https://doi.org/10.1111/1751-7915.70123
12. Valderrama MJ, González-Zorn B, De Pablo PC et al (2018) Educating in antimicrobial resistance awareness: adaptation of the Small World Initiative program to service-learning. FEMS Microbiol Lett 365:161. https://doi.org/10.1093/FEMSLE/FNY161
13. Blin K, Shaw S, Augustijn HE et al (2023) antiSMASH 7.0: new and improved predictions for detection, regulation, chemical structures and visualisation. Nucleic Acids Res 51:W46–W50. https://doi.org/10.1093/NAR/GKAD344

14. Gabant P, Borrero J (2019) PARAGEN 1.0: A Standardized Synthetic Gene Library for Fast Cell-Free Bacteriocin Synthesis. Front Bioeng Biotechnol 7. https://doi.org/10.3389/FBIOE.2019.00213
15. Sevillano E, Lafuente I, Peña N et al (2024) Isolation, Genomics-Based and Biochemical Characterization of Bacteriocinogenic Bacteria and Their Bacteriocins, Sourced from the Gastrointestinal Tract of Meat-Producing Pigs. Int J Mol Sci 25:12210. https://doi.org/10.3390/IJMS252212210
16. Waterhouse AM, Procter JB, Martin DMA et al (2009) Jalview Version 2—a multiple sequence alignment editor and analysis workbench. Bioinformatics 25:1189–1191. https://doi.org/10.1093/BIOINFORMATICS/BTP033
17. Wilkins MR, Gasteiger E, Bairoch A et al (1999) Protein Identification and Analysis Tools in the ExPASy Server. Methods Mol Biol 112:531–552. https://doi.org/10.1385/1-59259-584-7:531
18. Abramson J, Adler J, Dunger J et al (2024) Accurate structure prediction of biomolecular interactions with AlphaFold 3. Nature 2024 630:8016 630:493–500. https://doi.org/10.1038/s41586-024-07487-w
19. Pettersen EF, Goddard TD, Huang CC et al (2004) UCSF Chimera—A visualization system for exploratory research and analysis. J Comput Chem 25:1605–1612. https://doi.org/10.1002/JCC.20084
20. Kamilari E, O'Connor PM, de Farias FM et al (2025) Bacillus safensis APC 4099 has broad-spectrum antimicrobial activity against both bacteria and fungi and produces several antimicrobial peptides, including the novel circular bacteriocin safencin E. Appl Environ Microbiol 91. https://doi.org/10.1128/AEM.01942-24
21. Major D, Flanzbaum L, Lussier L et al (2021) Transporter Protein-Guided Genome Mining for Head-to-Tail Cyclized Bacteriocins. Molecules 26:7218. https://doi.org/10.3390/MOLECULES26237218
22. Vezina B, Rehm BHA, Smith AT (2020) Bioinformatic prospecting and phylogenetic analysis reveals 94 undescribed circular bacteriocins and key motifs. BMC Microbiol 20:1–16. https://doi.org/10.1186/S12866-020-01772-0
23. Xin B, Liu H, Zheng J et al (2020) In Silico Analysis Highlights the Diversity and Novelty of Circular Bacteriocins in Sequenced Microbial Genomes. mSystems 5:. https://doi.org/10.1128/MSYSTEMS.00047-20
24. Maqueda M, Sánchez-Hidalgo M, Fernández M et al (2008) Genetic features of circular bacteriocins produced by Gram-positive bacteria. FEMS Microbiol Rev 32:2–22. https://doi.org/10.1111/J.1574-6976.2007.00087.X
25. Hollmann A, Martinez M, Maturana P et al (2018) Antimicrobial peptides: Interaction with model and biological membranes and synergism with chemical antibiotics. Front Chem 6:363805. https://doi.org/10.3389/FCHEM.2018.00204
26. Travkova OG, Moehwald H, Brezesinski G (2017) The interaction of antimicrobial peptides with membranes. Adv Colloid Interface Sci 247:521–532. https://doi.org/10.1016/j.cis.2017.06.001

27. Krauson AJ, He J, Wimley AW et al (2013) Synthetic molecular evolution of pore–forming peptides by Iterative combinatorial library screening. ACS Chem Biol 8:823. https://doi.org/10.1021/CB300598K

Figures

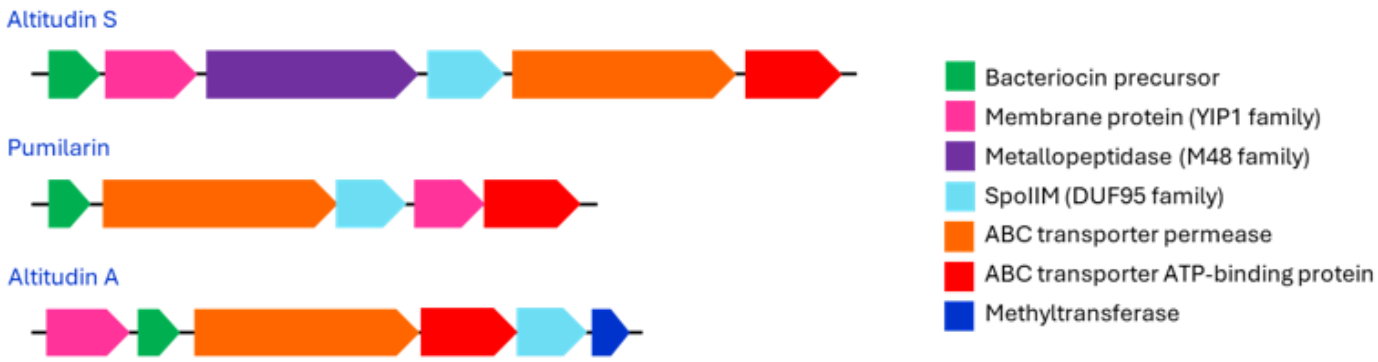


Figure 1

Genomic organization of the altitudin S BGC compared with those of pumilarin and altitudin in *B. altitudinis* ECC22. Genes are color-coded according to predicted function.

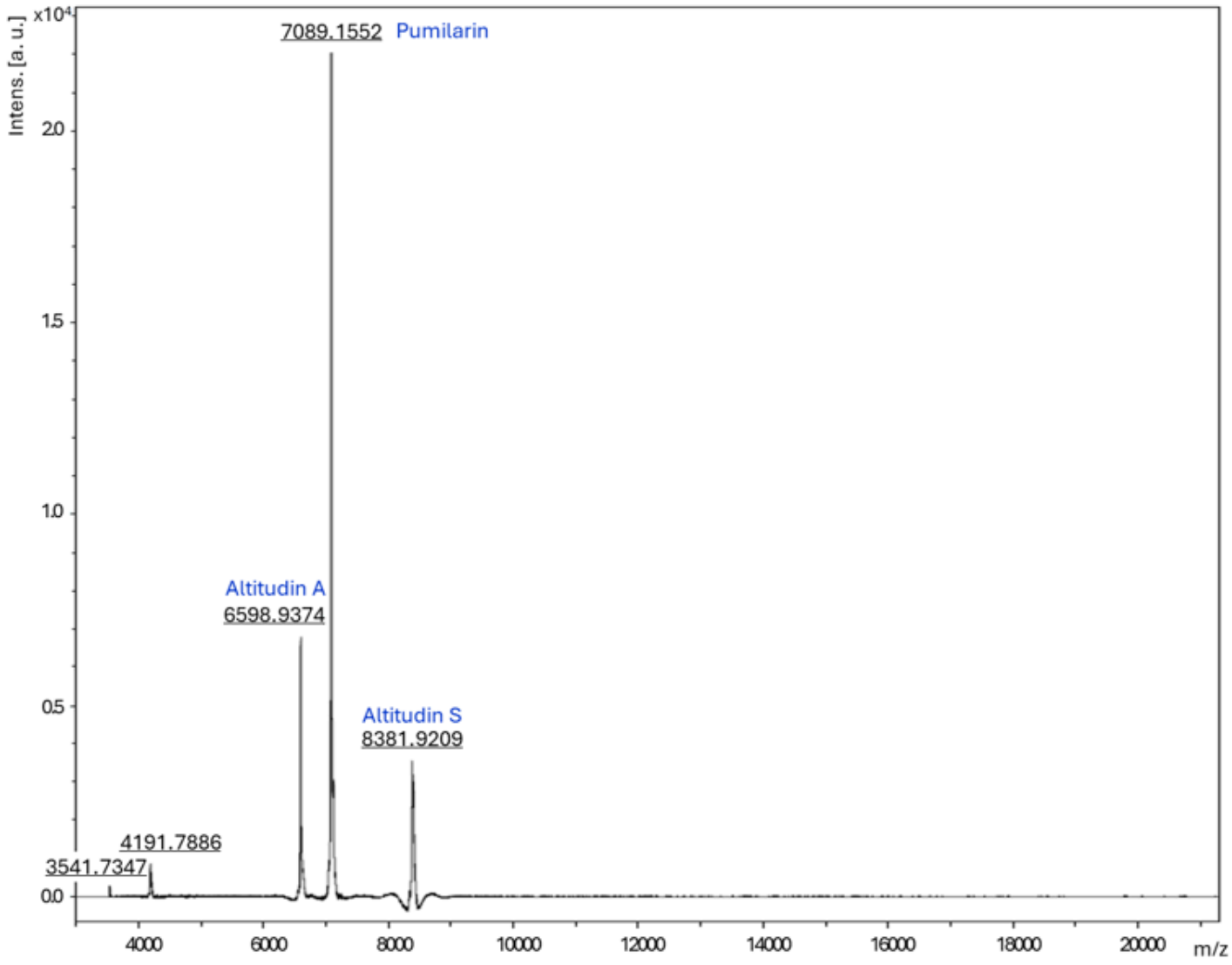


Figure 2

MALDI-TOF MS spectrum of the most active RP-FPLC fraction obtained from the purified CFS of *B. altitudinis* ECC22, showing peptide peaks corresponding to altitudin A (6598.9 Da), pumilarin (7089.1 Da), and the novel circular bacteriocin altitudin S (8381.9 Da).

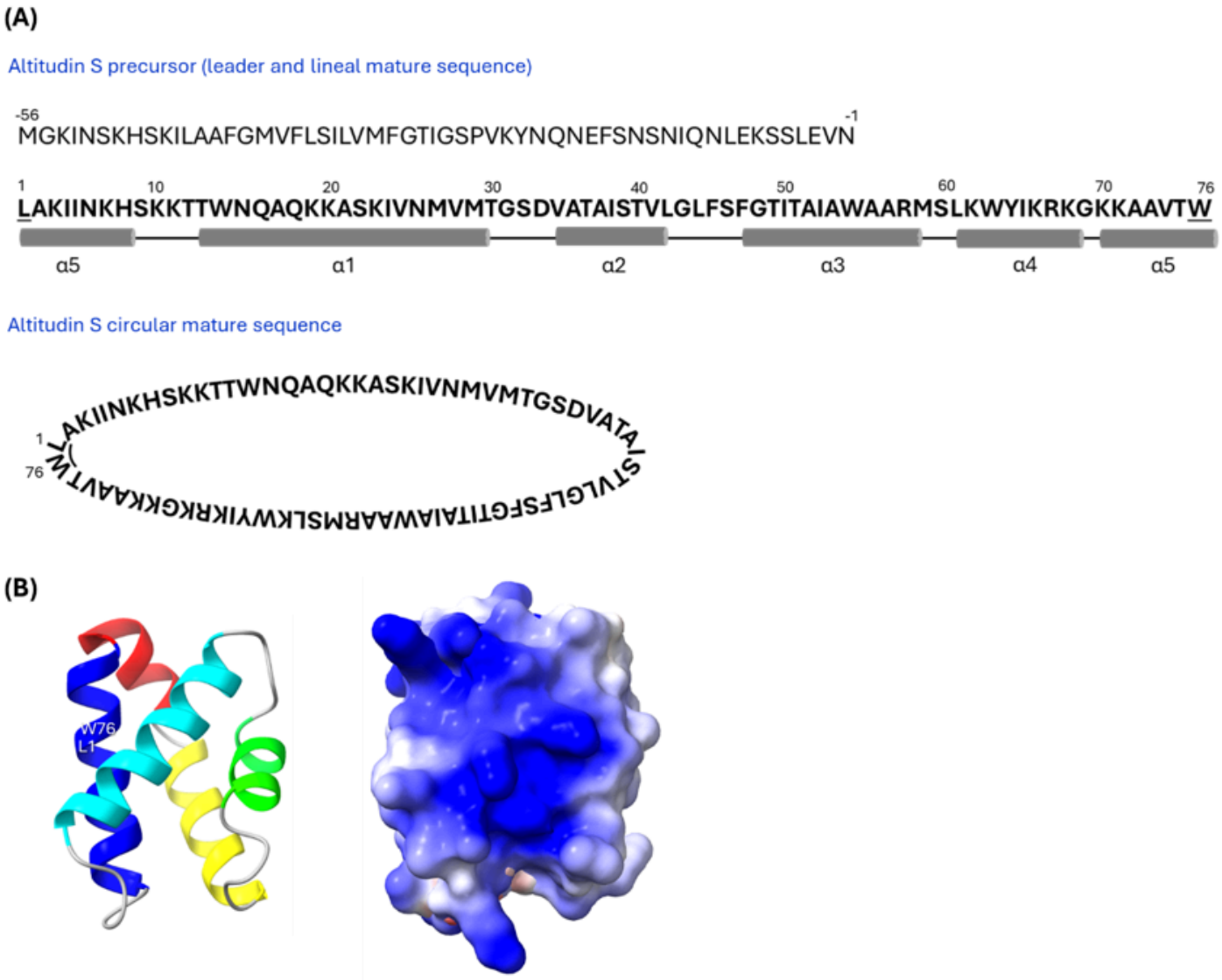


Figure 3

(A) Schematic representation of the altitudin S precursor peptide, consisting of a 56-residue leader sequence and a 76-residue mature peptide. The head-to-tail circularization junction (L1-W76) is underlined. Predicted α-helices within the mature sequence are shown in grey. **(B)**Predicted 3D structure of altitudin S generated using AlphaFold and visualized using ChimeraX. Left: cartoon representation highlighting the five α-helices. Right: electrostatic surface potential, colored red (negative), white (neutral), and blue (positive).

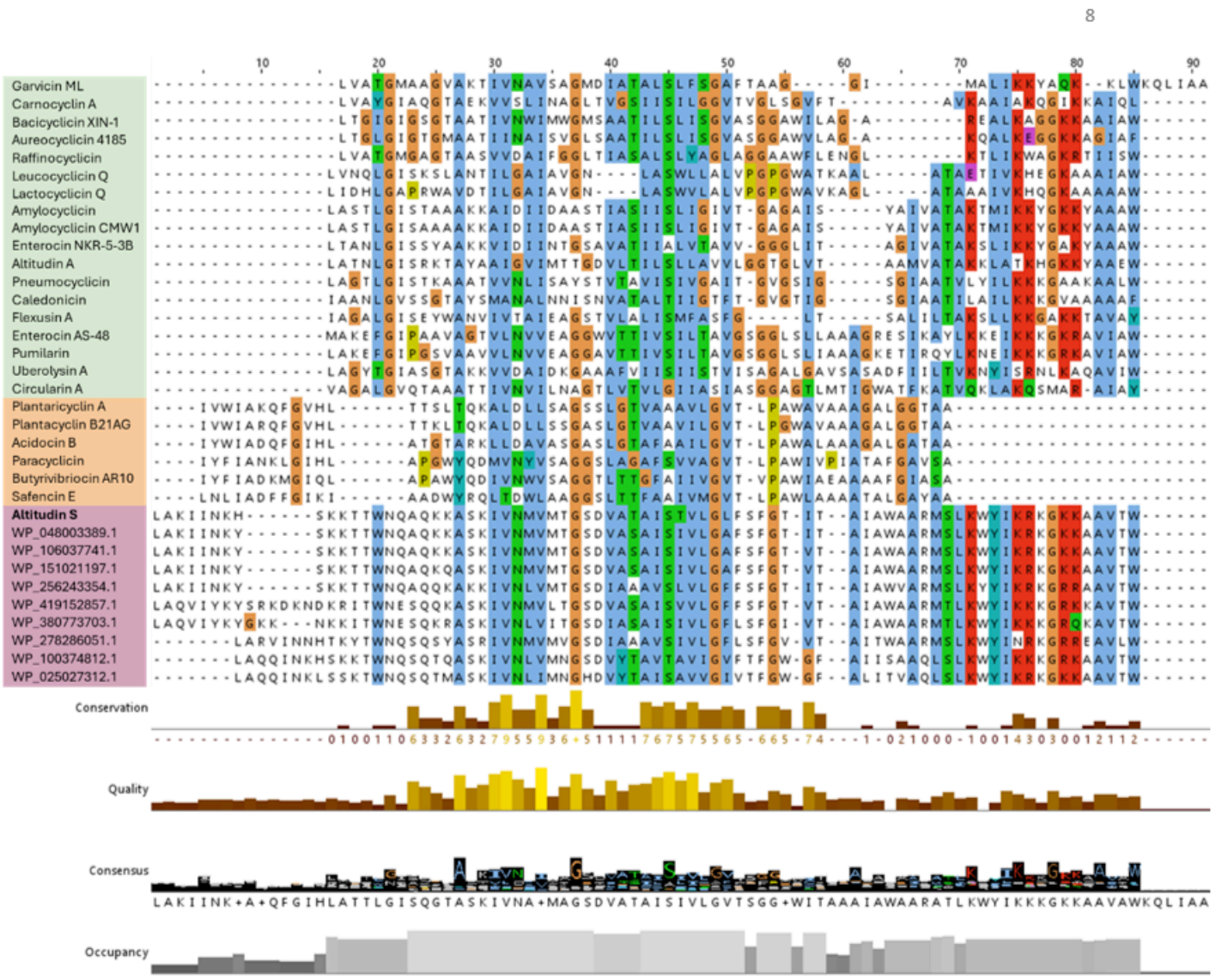


Figure 4

Multiple sequence alignment of altitudin S, its homologs, and representative circular bacteriocins. Mature peptide sequences from subgroup I (green box), subgroup II (orange box), and altitudin S with its homologs (purple box) were aligned using Clustal Omega implemented in Jalview (v.2.11.4.1) [16]. Amino acids are colored according to the Clustal scheme: blue (hydrophobic), green (polar), orange (small hydrophobic), and red (positively charged). Tracks below the alignment indicate conservation (residue conservation across sequences), alignment quality (reflecting confidence and physicochemical similarity), consensus sequence (shown as a sequence logo), and occupancy (proportion of non-gap residues at each position).

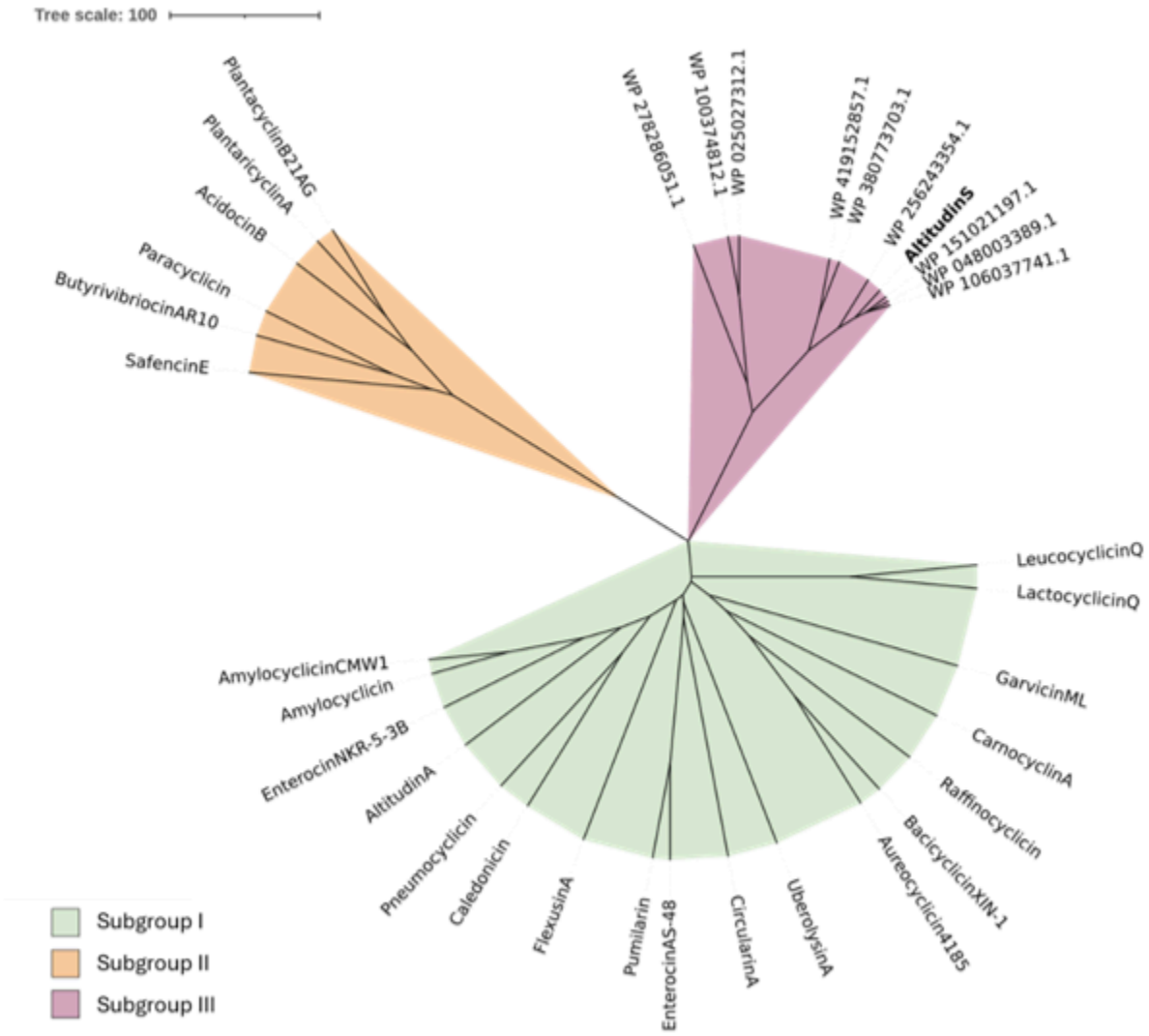


Figure 5

Phylogenetic analysis of circular bacteriocins. Phylogenetic tree based on the multiple sequence alignment of representative circular bacteriocins and altitudin S homologs. Alignments were generated using Clustal Omega, and the tree was constructed with the Neighbor-Joining method using the BLOSUM62 substitution matrix. Visualization was performed with iTOL (Interactive Tree of Life; https://itol.embl.de). Branch colors denote the three proposed subgroups: subgroup I (green), subgroup II (orange), and subgroup III (purple), the latter comprising altitudin S and its homologs.

Supplementary Files

This is a list of supplementary files associated with this preprint. Click to download.

- AltSProbioticsAntimicrob.Proteins31032026SIESG.docx